

pH-Responsive DNA-Binding Activity of *Helicobacter pylori* NikR[†]

Yanjie Li and Deborah B. Zamble*

Department of Chemistry, University of Toronto, Toronto, Ontario, Canada M5S 3H6

Received September 12, 2008; Revised Manuscript Received January 20, 2009

ABSTRACT: *Helicobacter pylori* NikR (HpNikR) is a nickel-responsive transcription factor. In addition to a role in nickel homeostasis, HpNikR is proposed to serve as a master activator–repressor for *H. pylori* acid adaptation by directly or indirectly regulating the expression of a battery of genes. One potential mechanism of this regulation is modulation of the DNA-binding activity of HpNikR by the decrease in internal pH that occurs upon exposure to acidic shock. To test this hypothesis, several properties of HpNikR were investigated under acidic conditions. At pH 5.8, the secondary and quaternary structures of the protein are not affected, and it still binds stoichiometric nickel in the same site, although with a slightly weaker affinity than that at pH 7.6. DNA-binding assays performed at pH 5.8 reveal that, in contrast to pH 7.6, HpNikR binds to the *ureA* promoter in a nickel-independent fashion. Binding to the *nikR* promoter at the lower pH is nickel dependent, however. Deletion of amino acids 3–11 of HpNikR abolished the nickel-responsive activity and enhanced nonspecific DNA binding. Site-directed mutagenesis of HpNikR indicates that either Asp7 or Asp8 in the N-terminus of HpNikR plays a part in the activation of DNA binding. Furthermore, Lys6 contributes selectively to complex formation with the *nikR* promoter sequence. The direct influence of pH on the activity of HpNikR may be critical to the role of this activator–repressor in the viability of *H. pylori*.

Helicobacter pylori (*H. pylori*¹) are gram-negative pathogenic bacteria that colonize the gastric mucosa of humans. More than 50% of the world population is infected by *H. pylori*, which are now accepted as a major cause of duodenal and gastric ulcers, as well as gastritis and certain types of gastric cancers (1). *H. pylori* multiply in a relatively narrow environmental pH range from 6.0 to 8.0 with optimal growth at close to neutral pH (2). However, in vivo this neutrophile has to cross through gastric acid (pH 1–2) to first reach the mucus layer and then reach the surface of the gastric epithelium (2, 3). Even after the initial colonization phase, *H. pylori* encounter considerable pH fluctuations that range as low as 1.0 during starvation to 6.0 in the digestive phase (2). When the external pH drops from 7.2 to 1.2 in the presence of urea, the apparent cytoplasmic pH of *H. pylori* cells drops from 7.5 to 5.4 (4).

To survive severe acid shock and to thrive in the mildly acidic environment of the human stomach, *H. pylori* have developed a variety of acid-adaptive mechanisms (2, 5). Central to the acid resistance of *H. pylori* is the urease enzyme that prevents a dramatic drop in the pH of the cytoplasm and periplasm of the bacteria by hydrolyzing urea

to produce ammonia (6). Urease has a dinuclear nickel cluster at the active site, and it is essential for the chronic colonization of the hostile environment in the human stomach (2, 6, 7). Another nickel enzyme that is required for efficient colonization by *H. pylori* is the [NiFe]-hydrogenase, which allows the bacteria to use hydrogen gas as an energy source (8) and has been linked to acid adaptation in other organisms (9, 10).

The nickel availability in *H. pylori*, which in turn constrains urease and hydrogenase activities, is controlled by a variety of transporters, metalloregulators, and auxiliary proteins (11–13). One of the key proteins in maintaining nickel homeostasis is *H. pylori* NikR (HpNikR), a nickel-responsive transcription factor that belongs to the ribbon–helix–helix (RHH) family of DNA-binding proteins (11, 14–16). Biochemical, genetic, and microarray studies demonstrate that HpNikR is a pleiotropic effector that controls both the activation and the repression of a variety of genes in response to nickel (14, 15, 17–22). For example, HpNikR is responsible for the nickel-dependent induction of urease expression (14), but it also acts as a repressor of various genes including its own (15). In addition to its role in nickel homeostasis, HpNikR has been implicated in the global response of *H. pylori* to acidic conditions (17, 18, 23). HpNikR controls acid-responsive gene expression in *H. pylori* via a regulatory circuit that functionally overlaps with the Fur regulator and possibly the Hp0166 regulator (17, 18, 23). This response, at least in part, may be due to increased nickel availability (17). Given the relatively low abundance of regulatory proteins in this organism (24), it is not surprising that the extant transcription factors such as HpNikR can respond to more than one type of signal. However, it is still

* To whom correspondence should be addressed. Phone/fax: (416) 978-3568. E-mail: dzamble@chem.utoronto.ca.

[†] This work was supported in part by funding from the Natural Sciences and Engineering Research Council (Canada), the Canadian Institutes of Health Research, and the Canada Research Chairs program.

¹ Abbreviations: DTNB, 5,5'-dithiobis(2-nitrobenzoic acid); DTT, dithiothreitol; *E. coli*, *Escherichia coli*; EDTA, ethylenediaminetetraacetic acid (disodium salt); EGTA, ethyleneglyco bis(1-aminoethyl-ether)-N,N,N',N'-tetraacetic acid; EMSA, electrophoretic mobility shift assay; IGEPAL, (octylphenoxy)polyethoxyethanol; *H. pylori*, *Helicobacter pylori*; SDS-PAGE, sodium dodecyl sulfate polyacrylamide gel electrophoresis; Tris, tris(hydroxymethyl)aminomethane.

not fully understood how HpNikR responds to dramatic changes in external environmental pH or how HpNikR distinctly regulates the individual genes under its control.

In this study we demonstrate that HpNikR exhibits pH-regulated DNA binding *in vitro* and that the effect of pH on the DNA-binding activity depends on the recognition sequence. Alignment of NikR sequences from different organisms reveals that HpNikR has additional amino acids at the N-terminus, and a recent study demonstrated that this region of HpNikR plays an important role in DNA recognition at a slightly alkaline pH (25). Similarly, our results suggest that Lys6 and one of two adjacent amino acids, Asp7 or Asp8, are critical for the specific responses of HpNikR. These observations afford new information on how HpNikR regulates multiple genes in response to pH changes as well as nickel availability.

EXPERIMENTAL PROCEDURES

Materials. All metal salts were purchased from Aldrich with 99.9% or higher purities. Restriction enzymes, kinases, and polymerases were obtained from New England Biolabs (Beverly, MA). Deoxyribonuclease (DNase) I was from Fermentas (Glen Burnie, MD). All other chemicals were molecular biology or analytical reagent grade.

Construction of Expression Vectors. The generation of pET24bhpnikr was described previously (26). The $\Delta 9$ aahpnikr gene was amplified from pET24bhpnikr plasmid by using the primers 5'-GACGATCATATGATCCGCTTTTCG-GTTTCTTTAC and 5'-GTATTTCTCGAGGCTATTCAT-TGTATTCAAAGC which exclude amino acids 3–11. The polymerase chain reaction (PCR) product was digested with the *Nde*I and *Xho*I restriction enzymes and ligated into the pET24b plasmid cut with the same enzymes to generate pET24b $\Delta 9$ aahpnikr. Site-directed mutagenesis was performed to prepare K6A, D7A, D8A, and D7A/D8A mutants according to the Quickchange site-directed mutagenesis protocol (Stratagene) by using primers listed in Table S1 of Supporting Information. All constructed plasmids were verified by DNA sequencing (ACGT Corporation, Toronto).

Protein Expression and Purification. HpNikR was expressed and purified as described previously (26). All mutants were expressed following the same procedure as for wild-type HpNikR except that the mutant proteins were induced overnight with 0.1 mM isopropyl- β -D-thiogalactopyranoside at 15 °C. The mutant proteins were purified by using the same procedure as wild-type HpNikR (26) with one modification. Following elution from a Ni-nitrilotriacetic acid column (Qiagen), a PD-10 gel filtration column (GE Healthcare) equilibrated with 20 mM Tris (pH 7.6) and 200 mM NaCl was used instead of dialysis to remove imidazole, EDTA, and DTT from the protein solutions before loading onto a MonoQ HR (10/10) fast protein liquid chromatography column (GE Healthcare). Protein concentrations were determined in 6 M guanidine hydrochloride (GHCl) and 5 mM EDTA (pH 7.6) by using a calculated extinction coefficient of $\epsilon_{280} = 9530 \text{ M}^{-1} \text{ cm}^{-1}$ (26). The purity of the proteins was assayed by sodium dodecyl sulfate polyacrylamide gel electrophoresis (SDS-PAGE). The oxidation state of the protein was routinely determined by using a 5,5'-dithiobis(2-nitrobenzoic acid) (DTNB) assay. In brief, protein samples and the standard curve of 7–56 μM β -mercapto-

ethanol were prepared in 6 M GHCl, 1 mM EDTA (pH 8), and 400 μM DTNB, and the absorbance was measured at 412 nm. The proteins with >95% purity and >95% reduction were used for subsequent experiments. The mass of each protein was determined by electrospray mass spectrometry (ESI-Qstar, Department of Chemistry, University of Toronto) and compared to the predicted values. The molecular weights of wild-type protein and mutants were as follows: HpNikR $\text{MW}_{\text{obs}} = 17146.2 \text{ Da}$ (predicted 17147.2 Da), $\Delta 9$ aa $\text{MW}_{\text{obs}} = 16162.0 \text{ Da}$ (predicted 16163.2 Da), D7A/D8A $\text{MW}_{\text{obs}} = 17058.0 \text{ Da}$ (predicted 17059.2 Da), D8A $\text{MW}_{\text{obs}} = 17102.0 \text{ Da}$ (predicted 17103.2 Da), D7A $\text{MW}_{\text{obs}} = 17104.0 \text{ Da}$ (predicted 17103.2 Da), and K6A $\text{MW}_{\text{obs}} = 17090.0 \text{ Da}$ (predicted 17090.2 Da). To confirm that the apo-proteins did not contain trace amounts of nickel or other transition metals, all apo-proteins were analyzed by a high-performance liquid chromatography assay as described previously (27), in which the process can be used following acid hydrolysis for the quantitative determination of the most prevalent biological transition metals.

Quaternary Structure Analysis. Sedimentation equilibrium experiments were performed in a Beckman XL-series analytical ultracentrifuge by using the absorbance optical system (Department of Biochemistry, University of Toronto). Apo-HpNikR (20, 40, 60 μM) in 20 mM potassium phosphate buffer, pH 7.6, and apo-HpNikR (25, 50, 75 μM) and holo-HpNikR (20, 40, 60 μM) in 20 mM potassium phosphate buffer, pH 5.8, were examined. The sedimentation equilibrium of the protein was performed at 15 000, 18 000, and 21 000 rpm at 20 °C. In addition, the apo- and holo-HpNikR at pH 7.6 were confirmed to be tetramers in solution (28, 29) by using size-exclusion chromatography on a Superdex 200 high load 26/60 gel filtration column (GE Healthcare).

Circular Dichroism (CD). CD spectra were recorded on an Olis DSM 1000 CD spectrophotometer at 20 °C. The protein concentrations were 20 μM in 20 mM potassium phosphate buffer, pH 7.6 or 5.8. A total of five spectra were obtained and averaged to obtain the final spectrum. The mean residue ellipticity $[\theta]$ ($\text{deg} \cdot \text{cm}^2 \cdot \text{dmol}^{-1}$) was obtained by normalization of the measured ellipticity (θ , mdeg), using $[\theta] = (\theta \times 100)/(nlc)$, where n is the number of residues (148 for HpNikR, K6A, D7A, D8A, and D7AD8A, 139 for $\Delta 9$ aaHpNikR), c is the total concentration (mM), and l is the cell path length (cm).

Metal Analysis and EGTA Competition. Electronic absorption spectra were collected at 25 °C on an Agilent 8453 spectrophotometer equipped with an 89090 Peltier temperature controller. Both nickel titration and EGTA competition experiments were performed with separate aliquots of protein incubated overnight at 4 or 25 °C. For the competition assays, samples containing 20 μM HpNikR or mutant proteins in 20 mM potassium phosphate, pH 7.6 or pH 5.8, were incubated with 2 mM EGTA and various concentrations of Ni^{2+} . The fraction of Ni(II) -HpNikR was calculated by using the extinction coefficient measured with a nickel titration in the absence of competitor, and the concentration of free nickel was calculated as previously described (26). The K_d of Ni-EGTA was calculated according to the experimental pH and ionic strength and for pH 7.6 and pH 5.8 in the presence of 0.1 M NaCl is $5.21 \times 10^{-11} \text{ M}$ and $6.32 \times 10^{-8} \text{ M}$, respectively. The data were fit to a Langmuir equation

with a variable Hill coefficient n : $r = [\text{Me}]^n / (K_{\text{d(app)}}^n + [\text{Me}]^n)$, where r is the fraction of protein bound to metal and $K_{\text{d(app)}}$ represents the free metal concentration required for 50% binding. All reported data are the average of at least three independent experiments.

Electrophoretic Mobility Shift Assays (EMSAs). EMSAs were performed with 7% native polyacrylamide gels containing 300 mM boric acid and 75 mM Tris-HCl (pH 7.5) with 800 μM NiSO_4 . The same boric-Tris solution containing the same concentration of NiSO_4 was used as running buffer. The binding buffer was composed of 20 mM Tris-HCl (pH 7.5), 100 mM KCl, 3 mM MgCl_2 , 0.1% IGEPAL, 5% glycerol, and 0.1 mg/mL sonicated herring sperm DNA (Promega).

The DNA oligonucleotides described previously (26) from the *ureA* (204 bp) and *nikR* (203 bp) promoters were amplified from pPC163hyureA or pPC163NikRprom plasmids by PCR. The product DNA was purified from an agarose gel by using a DNA extraction kit (Qiagen). Purified DNA was labeled at both ends with γ - ^{32}P -adenosine-5'-triphosphate by using T4 polynucleotide kinase. Unincorporated nucleotides were removed by a G-25 microspin column (GE Healthcare). The amount of labeling was determined by scintillation counting on a Packard Tri-Carb 2900 TR LSC.

Around 10 fmol of radiolabeled DNA (~ 5000 cpm) was incubated with the indicated concentrations of HpNikR or mutant proteins for 30 min at 25 °C in 50 μL of binding buffer as noted above. All reaction solutions were resolved on the 7% native polyacrylamide gel at 350 V, 4 °C. The gel was vacuum-dried and exposed overnight to a phosphor screen, which was scanned on a Molecular Dynamics Storm 860 phosphorimager and analyzed with ImageQuant 5.0 software. The fraction of DNA bound was determined by measuring the radioactive intensity of free (unbound) DNA versus that of the total DNA. Some of the data were better fit to the Hill equation in which n is allowed to vary: $r = [\text{P}]^n / (K_{\text{d}}^n + [\text{P}]^n)$ where r is the fraction of DNA bound to protein and K_{d} is the protein concentration required for 50% DNA binding. However, given the tetrameric structure of HpNikR and in analogy with the *E. coli* NikR, it is likely that HpNikR is a tetramer both in solution and bound to DNA (30–33), so it is unclear at this time how any cooperativity could be a component of DNA binding. When n was fixed as 1 (i.e., using the Langmuir isotherm $r = [\text{P}] / (K_{\text{d}} + [\text{P}])$), the values for K_{d} did not change more than 20%, and these are the values that are reported.

DNase I Footprinting Assays. To prepare oligonucleotides with a radiolabel on only one strand, the ^{32}P -labeled DNA probes described above for the EMSAs were digested by *Sal*I (*ureA* promoter) or *Apo*I (*nikR* promoter). The digested products were resolved on a 7% native polyacrylamide gel, and the expected band was cut out of the gel and electroeluted at 150 V for 1 h followed by ethanol precipitation. The amount of labeling was determined by scintillation counting. To confirm that the correct DNA sequences were obtained and to localize the footprint, the Maxam–Gilbert chemical G reaction was performed as described (34).

pH 7.6 Reaction. Reactions were carried out in 20 μL solutions containing 100 mM KCl, 20 mM Tris (pH 7.6), 1 mM MgCl_2 , 1 mM CaCl_2 , 5% (v/v) glycerol, and the indicated concentrations of HpNikR or mutant proteins. After

the probes (~ 50 fmol, 30 000 cpm per sample) were added, the samples were incubated at 25 °C for 30 min. Then 1 μL of freshly diluted 2 $\mu\text{g/mL}$ DNase I (100 mM KCl, 20 mM Tris, pH 7.6, 1 mM MgCl_2 and 1 mM CaCl_2) was added into each sample. The reactions were quenched after 4 min by adding 80 μL of DNase I stop buffer (20 mM Tris, pH 8, 40 mM EDTA pH 8, 1% (w/v) SDS, and 0.1 $\mu\text{g/mL}$ herring sperm DNA). Proteins were removed by extraction with 100 μL of 24:25:1 phenol:chloroform:isoamyl alcohol. The DNA was precipitated with 2.5 vol of ethanol at -20 °C overnight. After centrifugation, the pellets were dried by centrifugation under vacuum, resuspended in 4 μL of formamide loading buffer, and denatured at 90 °C for 5 min. Samples were then loaded onto an 8% denaturing polyacrylamide gel that was prerun to 50 °C. The gel was run at about 2 000 V and 50 °C and then vacuum-dried and exposed overnight to a phosphor screen, which was scanned on a Molecular Dynamics Storm 860 phosphorimager and analyzed with ImageQuant 5.0 software. The percentages of bound DNA were calculated by measuring the radioactive intensity of a disappearing band versus the radioactive intensity of a strong nonprotected band. Multiple bands were analyzed for each gel, and all reported affinities are the average of the data from at least two independent experiments.

pH 5.8 Reaction. $\Delta 9\text{aa}$ and D7A/D8A tended to aggregate upon titration with nickel at pH 5.8. Protein aggregation at pH 5.8 was monitored by measuring light scattering on a fluorometer (Jobin Yvon) with λ_{ex} and λ_{em} both set at 500 nm and slit widths set at 2 nm. Protein aggregation was not detected with less than 1 μM protein (data not shown), so all DNase I footprinting reactions with these mutant proteins at pH 5.8 were performed with less than 1 μM . The whole process was the same as the reaction performed at pH 7.6 except that 20 mM potassium phosphate buffer (pH 5.8) was used instead of the Tris buffer. DNase I footprinting reactions with 20 mM phosphate buffer at pH 7.6 were also performed for comparison and did not produce results different from those performed in Tris buffer at the same pH (data not shown).

RESULTS

When *H. pylori* are exposed to acidic conditions of pH 1, the pH_{in} is proposed to drop to between 5.8 and 4.9 (4, 35), although there is some uncertainty as to how much the intracellular pH varies and how it is modulated. Most previous biochemical studies focused on the metal- and DNA-binding properties of HpNikR at pH values from 8.8 to 6.5 (19, 21, 25, 26, 28, 36–39). To understand how this master activator–repressor could contribute to the response of *H. pylori* to acidic shock and the ensuing decrease in cytoplasmic pH, several activities of HpNikR were investigated at pH 5.8. This pH was chosen because it is within the range of internal pH measured in *H. pylori* after an acid shock (35). Also, it is slightly higher than the pI of HpNikR (~ 5.2), so protein precipitation is avoided.

HpNikR Secondary and Quaternary Structures at pH 7.6 and 5.8. To investigate the effects of nickel binding and pH on the secondary structure of HpNikR, CD experiments were performed. The overall spectra are typical for globular proteins and have features resulting from a mix of α -helices and β -sheets (Figure 1A). Stoichiometric nickel per protein

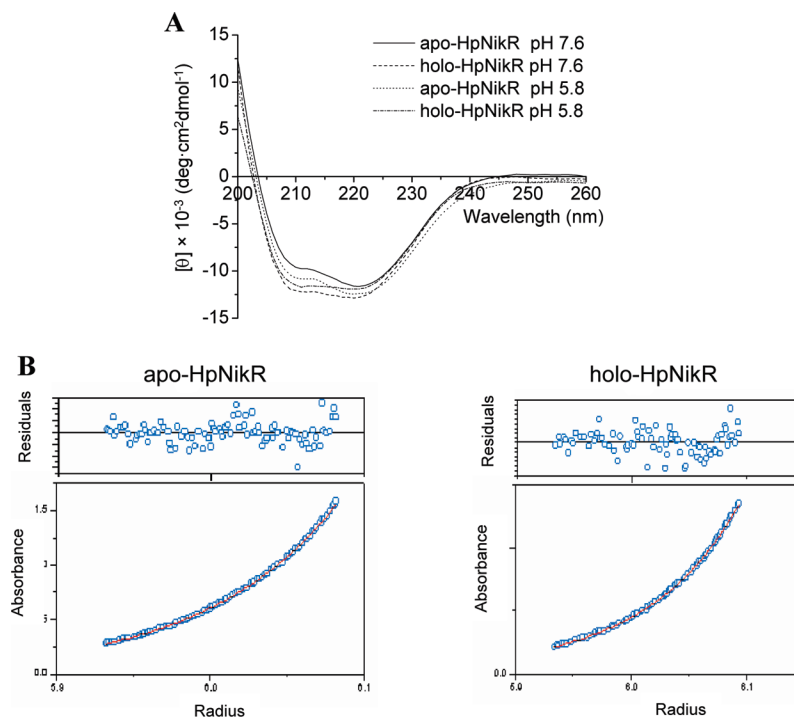


FIGURE 1: HpNikR secondary and quaternary structure at pH 7.6 and pH 5.8. (A) CD spectra of 20 μM apo- and Ni(II)-HpNikR in 20 mM phosphate buffer at pH 7.6 and pH 5.8 at 20 $^{\circ}\text{C}$. (B) Analytical ultracentrifugation data of both apo- and holo-HpNikR at pH 5.8 are fit to a tetramer model.

monomer induces a small increase in secondary structures at pH 7.6, in agreement with previous studies (36, 37). The CD spectra of HpNikR at pH 5.8 in the absence or presence of 1 equiv of nickel are very similar to those at pH 7.6. The introduction of the K6A, D7A, or D8A mutations (discussed below) did not affect the secondary structure of the apo- or holo-protein at either pH (data not shown). The $\Delta 9\text{aa}$ and D7A/D8A mutants exhibit similar secondary structure as HpNikR at pH 7.6, as do the apo-proteins at pH 5.8. However, as a result of the aggregation of holo- $\Delta 9\text{aa}$ and holo-D7A/D8A at pH 5.8 at the concentrations needed to obtain a CD spectrum, these mutants could not be examined by using this method.

The quaternary structures of apo- and holo-HpNikR at pH 7.6 were investigated by size-exclusion chromatography, and the results indicate that both apo- and holo-HpNikR are tetramers at a neutral pH as previously reported (data not shown) (28, 29). Analytical ultracentrifugation revealed that both apo- and holo-HpNikR are also tetramers at pH 5.8 (Figure 1B), which is consistent with the quaternary structure observed in the crystal structures obtained at pH 4.6 (32) and suggests that a tetramer is likely the functionally active form of the protein.

Stoichiometric Nickel Binding at pH 7.6 and pH 5.8. As observed at pH 7.6 (26), titration of HpNikR with nickel at pH 5.8 produced a change in the electronic absorption spectrum with a maximum absorption at 302 nm that saturated upon the addition of 1 equiv of nickel per monomer (Figure 2A), indicating quantitative nickel binding at this lower pH as previously reported (29). The lack of change in the difference spectrum suggests that, at pH 5.8, the nickel is bound to the same highly conserved nickel-binding site as at pH 7.6 (26, 30, 40, 41). To determine the affinity of HpNikR for Ni(II) at pH 5.8, the protein was titrated with nickel in the presence of the competitor EGTA (Figure 2B),

and although problems with protein precipitation precluded reaching complete saturation, 50% saturation was achieved at $(1.6 \pm 0.1) \times 10^{-9}$ M nickel (Figure 2B). This nickel affinity is weaker than that measured at pH 7.6, $(3.0 \pm 0.3) \times 10^{-12}$ M (26), which is expected given that the binding site is composed of three histidines and one cysteine (32, 40), and at the lower pH the competition between the nickel ions and protons for these ligands would be greater. A similar decrease in nickel-binding affinity upon reducing the pH from 8.0 to 6.5 was also observed in isothermal titration calorimetry (ITC) experiments with HpNikR, although different binding constants were reported (37). At pH 8.0, ITC data suggested that two nickel ions bind to the HpNikR tetramer with $K_D \sim 0.5$ nM and that two more bind with $K_D \sim 6$ nM, whereas at pH 6.5, the sequential dissociation constants increase to ~ 12 nM and ~ 160 nM, respectively (37). Furthermore, it has been noted that several other nickel metalloproteins also have weakened binding affinities at an acidic pH (29, 42, 43).

Nickel titration of the mutant proteins revealed electronic absorption signals similar to that observed for wild-type protein and saturation with 1 equiv of nickel per monomer (Supporting Information, Figure S1b). The molar extinction coefficients determined from a direct Ni^{2+} titration were used to calculate the nickel affinities at pH 7.6 in an EGTA competition (data not shown), revealing 50% saturation at the same magnitude of free nickel concentrations as that of wild-type protein (10^{-12} M). At pH 5.8, the affinity for nickel of mutants K6A, D7A, and D8A is similar to that of wild-type as well, but because of aggregation the nickel affinities of Ni(II)- $\Delta 9\text{aa}$ and Ni(II)-D7A/D8A at pH 5.8 were not determined.

Ni^{2+} -Responsive DNA Binding to the *ureA* and *nikR* Promoters. As previously reported, HpNikR binding to the *ureA* promoter in the presence of nickel at

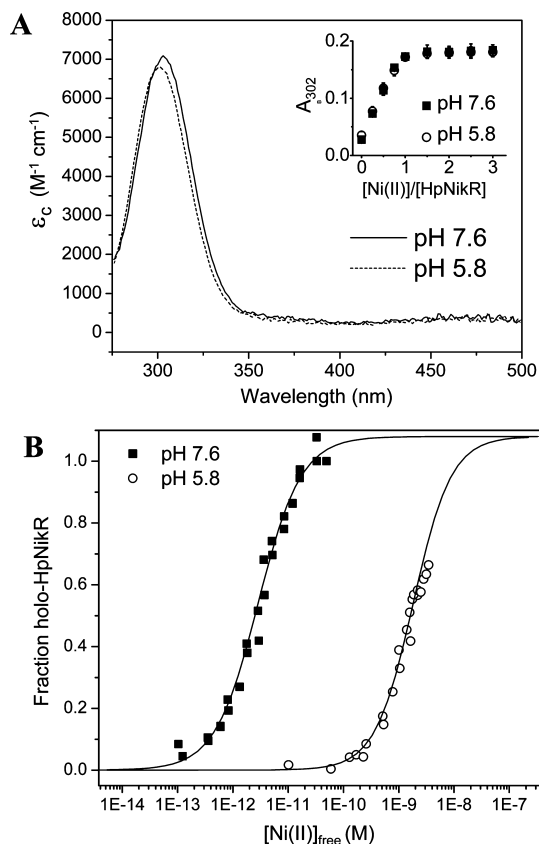


FIGURE 2: Nickel binding to HpNikR at pH 7.6 and pH 5.8. (A) Difference electronic absorption spectra of nickel bound to HpNikR at pH 7.6 and pH 5.8. Inset: titration of 20 μM HpNikR with increasing amounts of nickel at pH 7.6 or pH 5.8 reveals saturation with 1 equiv of metal per monomer. (B) The nickel affinity of HpNikR at pH 7.6 and pH 5.8 was determined by titrating the protein with NiSO_4 in the presence of 2 mM EGTA at pH 7.6 and pH 5.8. The increase of absorbance at 302 nm was monitored, and the fraction of Ni(II)-HpNikR was calculated as described in Experimental Procedures, as was the concentration of free nickel. The data were compiled from three separate experiments and were fit to a Hill equation to calculate a concentration of nickel required for half-saturation of $(3.0 \pm 0.3) \times 10^{-12}$ M with $n = 1.2 \pm 0.2$ at pH 7.6 and $(1.6 \pm 0.1) \times 10^{-9}$ M with $n = 1.3 \pm 0.1$ at pH 5.8.

Table 1: Apparent DNA-Binding Affinities ($\times 10^8$ M) Calculated from Mobility Shift Assays Performed at pH 7.6^a

	wild type	$\Delta 9\text{aa}$	D7AD8A	D7A	D8A	K6A
<i>ureA</i>	1.9 ± 0.6	5.5 ± 1.2	2.6 ± 0.2	2.7 ± 0.4	2.4 ± 1.7	5.0 ± 1.7
<i>nikR</i>	133 ± 36	3.6 ± 0.5	7.6 ± 2.4	41.6 ± 9.9	77.4 ± 42.0	$>1000^b$

^a Data were fit to a Langmuir isotherm. The affinities reported are the concentrations of protein needed to reach 50% saturation ($\times 10^8$ M) and represent the average of at least three independent experiments ± 1 standard deviation. ^b No clear shift is observed with up to 10 μM K6A, so the affinity is estimated to be above this protein concentration.

pH 7.6 was observed by using EMSAs (Table 1) (19, 25, 26, 36, 38), and holo-HpNikR produced a clear footprint on the *ureA* promoter in DNase I footprinting assays (Table 2) (19, 25, 26, 28, 38). In contrast, although HpNikR binding to the *nikR* promoter in the presence of nickel is observed at pH 7.6 or 8.8 by using EMSAs (Table 1) (15, 25, 26), no footprint with holo-HpNikR could be detected on the *nikR* promoter in the DNase I footprinting assay, either with or without 100 μM excess Ni^{2+} (Figure 3A). It is possible that the weaker affinity for the *nikR* promoter ($\sim 1 \mu\text{M}$, Table 1) may result in a half-life of

the HpNikR-*nikR* complex that is too short to be detected in the DNase I footprinting assay, but attempts to detect a footprint by varying the incubation time with DNase I were not successful (data not shown).

Given that the intracellular pH of *H. pylori* is affected by the extracellular pH (4, 35), it is possible that the DNA-binding properties of HpNikR are affected by the cytoplasmic pH change, as observed for other transcription factors (44–46). For this reason, binding to the *ureA* and *nikR* promoters was examined at pH 5.8 by using the DNase I footprinting assay. In contrast to the experiments performed at pH 7.6, at pH 5.8, a clear footprint was observed with ~ 100 nM holo-HpNikR on the 203-bp *nikR* oligonucleotide (Figure 3B). In addition, two hypersensitive bands corresponding to positions -1 and -2 relative to the transcription start site were observed in the presence of 1 μM holo-HpNikR (Figure 3B), indicating an increase in accessibility to cleavage by DNase I. Such hypersensitive bands, which are not observed in the footprint on the *ureA* promoter, suggest that the structure of the *nikR* promoter DNA is distorted in the complex with HpNikR at pH 5.8. No change in the binding of holo-HpNikR to the *nikR* promoter at pH 5.8 was observed upon addition of excess 100 μM Ni^{2+} or 800 μM Ni^{2+} (Figure 3B and data not shown), and no footprint was observed with up to 10 μM apo-HpNikR at pH 5.8.

The experiments with the *ureA* promoter at pH 5.8 revealed a different trend than with *nikR*. Although binding to the *ureA* promoter was observed at pH 7.6 only in the presence of nickel, at pH 5.8 a footprint was detected both in the presence and the absence of nickel (Figure 3C). Both apo- and holo-HpNikR bind to the *ureA* promoter at pH 5.8 at the same binding site and with similar affinities as observed for the holo-protein at pH 7.6 ($\sim 10^{-8}$ M, Figure 3C and Table 2).

To determine the specificity of DNA binding at pH 5.8, herring sperm DNA was titrated into the DNase I footprinting samples (Supporting Information, Figure S2). This additional DNA resulted in an overall decrease in DNase I cleavage of the labeled probes, but even in the presence of over 1000-fold excess nonspecific DNA (by mass), HpNikR still binds to *ureA* (apo- and holo-protein) and *nikR* (holo-protein) promoters with relatively high affinities ($\sim 10^{-8}$ M and $\sim 10^{-7}$, respectively) at a specific region.

Deletion of the N-Terminus of HpNikR. An alignment of the HpNikR sequence with NikR homologues from other organisms reveals that HpNikR has several extra amino acids at the N-terminus (Figure S3, Supporting Information), a region that is not ordered in the X-ray crystal structure of the protein (32). To test whether this N-terminal sequence is important for DNA binding to the *nikR* or *ureA* sequences, the mutant $\Delta 9\text{aa}$ was prepared by removing residues 3–11 (TPNKDDSI). EMSAs at pH 7.6 with this mutant revealed the same binding affinity as that of wild-type HpNikR on the *ureA* promoter ($\sim 10^{-8}$ M) but a much tighter affinity for the *nikR* promoter (Table 1). This result suggests that amino acids 3–11 play an important role in the HpNikR-*nikR* promoter interaction. While this work was in progress, a study of an HpNikR mutant lacking amino acids 2–10 reported the same trend by using EMSAs at pH 8.8, and experiments with multiple oligonucleotide sequences demonstrated that the extra N-terminal sequence of HpNikR

Table 2: Apparent DNA-Binding Affinities ($\times 10^8$ M) of HpNikR and Mutants for the *ureA* and *nikR* Promoters Measured in DNase I Footprinting Assays^a

	wild type		$\Delta 9aa$		D7AD8A		D7A		D8A		K6A	
	apo	holo	apo	holo	apo	holo	apo	holo	apo	holo	apo	holo
pH 7.6												
<i>ureA</i>	n/d ^b	6 ± 1	3 ± 1	3 ± 1	2.0 ± 0.1	1.4 ± 0.1	n/d	3 ± 1	n/d	2 ± 1	n/d	16 ± 2
<i>nikR</i>	n/d	n/d	nonspecific ^c		nonspecific		n/d	n/d	n/d	n/d	n/d	n/d
pH 5.8												
<i>ureA</i>	2.5 ± 0.9	2.8 ± 0.4	nonspecific		nonspecific		0.9 ± 0.1	0.8 ± 0.1	2.7 ± 0.4	2.6 ± 0.5	2.7 ± 0.4	3.9 ± 0.2
<i>nikR</i>	n/d	12 ± 3	nonspecific		nonspecific		n/d	2.0 ± 0.3	n/d	4 ± 1	n/d	n/d

^a Calculated from DNase I footprinting experiments at pH 7.6 and pH 5.8. The data were fit to the Langmuir isotherm, and the affinities reported are the concentrations of protein needed to reach 50% saturation ($\times 10^8$ M) and represent the average of at least two independent experiments ± 1 standard deviation. ^b A footprint was not detected. ^c Nonspecific indicates delocalized footprint.

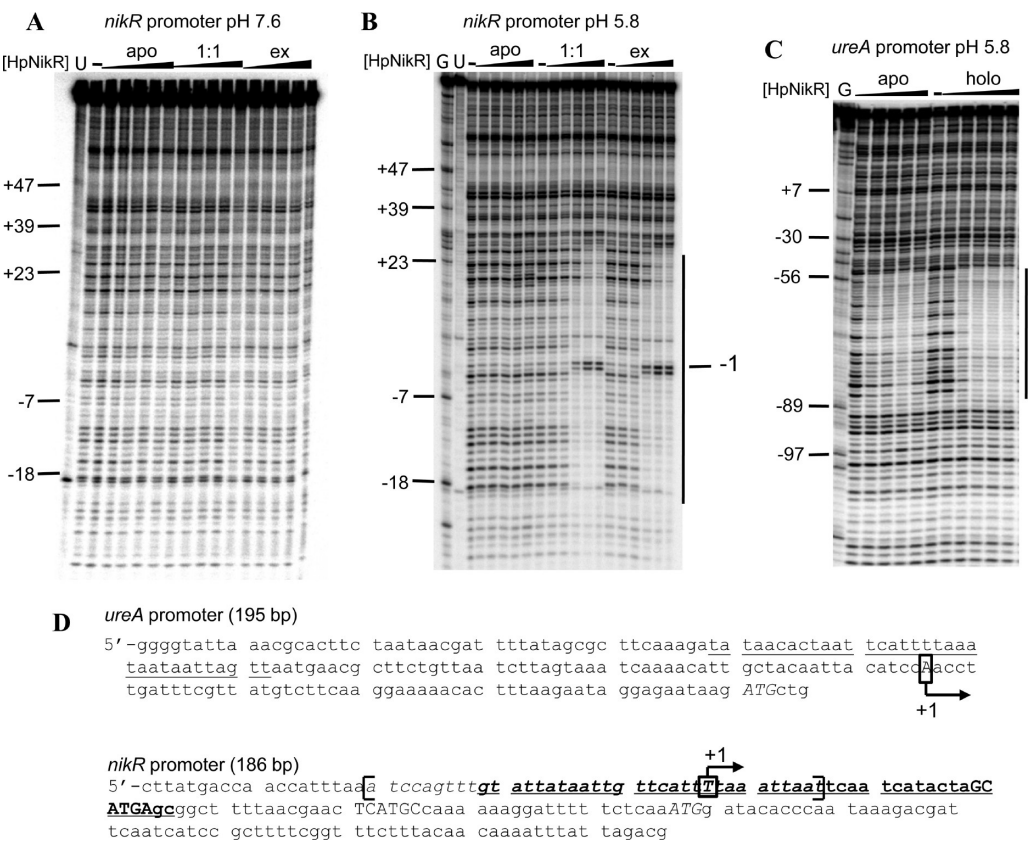


FIGURE 3: DNA binding to the *nikR* and *ureA* promoters. DNase I footprinting on a 186-bp *nikR* probe with apo-HpNikR, holo-HpNikR, or holo-HpNikR in the presence of 100 μ M excess nickel at (A) pH 7.6 or (B) pH 5.8. The protein (10 nM, 100 nM, 1 μ M, 5 μ M, and 10 μ M) was incubated with the DNA for 30 min prior to the addition of DNase I and analysis on an 8% denaturing polyacrylamide gel. G indicates a Maxam–Gilbert G reaction, and the numbering of the nucleotides are with respect to the transcription start site (28). U indicates the uncut DNA. (C) DNase I footprinting of apo-HpNikR and holo-HpNikR on a 195-bp *ureA* probe at pH 5.8. The footprint is in the same location as previously reported at pH 7.6 (26). (D) DNA sequences of the *ureA* and *nikR* probes. The protected regions in the DNase I footprinting experiments are underlined, and the transcription start sites are boxed. The bracketed sequence on the *nikR* promoter is the binding site determined in a previous study by using HpNikR with three extra amino acids at the N-terminus (28). The six-base half-sites of the inverted repeat similar to the *E. coli* NikR recognition sequence are in uppercase.

is required to prevent the protein from binding to low-affinity and nonspecific DNA sequences (25). To examine the role of the N-terminus of HpNikR further, DNase I footprinting assays at pH 7.6 were performed to determine the location of the $\Delta 9aa$ binding sites on the *ureA* and *nikR* promoters. On the 195-bp *ureA* oligonucleotide, holo- $\Delta 9aa$ binds with a similar affinity (Table 2) and in the same location as the full-length protein (Figure 4A). However, removal of the N-terminal arm eliminated the nickel dependence of complex formation with the *ureA* sequence because the apoprotein

produces the same footprint. In addition, an extended footprint is observed on the *ureA* promoter at higher concentrations of the $\Delta 9aa$ protein (~ 370 nM) at pH 7.6 (Figure 4A), which is consistent with the slower mobility of the DNA complex observed in the EMSAs (Figure S4a, Supporting Information). Similarly, DNase I footprinting with $\Delta 9aa$ on the *nikR* promoter revealed that although holo- $\Delta 9aa$ binding to the *nikR* promoter is observed at pH 7.6, in contrast to wild-type protein, it is only with a delocalized binding site (Figure 4B), which is also consistent with the higher mobility band observed in the

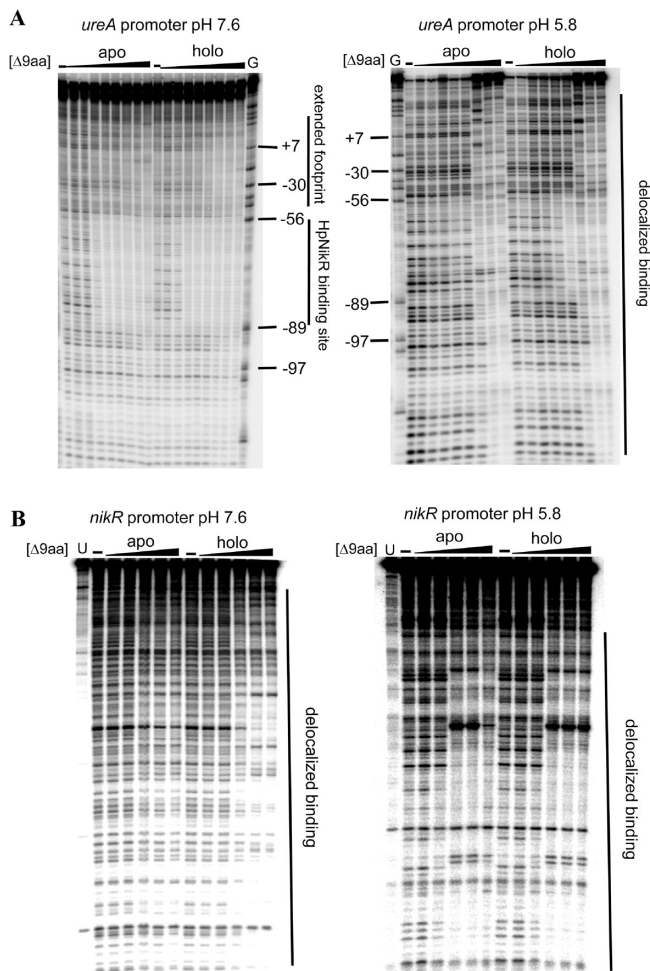


FIGURE 4: $\Delta 9aa$ binding to the *ureA* and *nikR* promoter at pH 7.6 and pH 5.8. (A) Apo- or holo- $\Delta 9aa$ was incubated with the *ureA* promoter at pH 7.6 (diluted 1/3 in successive samples from 10 μ M to 4 nM; left) or pH 5.8 (diluted 1/3 in successive samples from 1 μ M to 1 nM; right). (B) $\Delta 9aa$ (from 1 μ M to 12 nM, diluted 1/3 in successive samples) was incubated with the *nikR* promoter at pH 7.6 (left) and pH 5.8 (right). The protein was incubated with the indicated DNA for 30 min prior to the addition of DNase I and analysis on 8% denaturing polyacrylamide gels. G indicates a Maxam–Gilbert G reaction, and the numbers of the bases are with respect to the transcription start site. U indicates the uncut DNA.

EMSAs (Figure S4b, Supporting Information). The larger areas of protection caused by $\Delta 9aa$ observed in our DNase I assays provide more evidence for the proposed role of the N-terminus in sequence-selective DNA recognition (25).

DNase I footprinting of $\Delta 9aa$ with *ureA* and *nikR* promoters were also performed at pH 5.8. The results reveal that both apo- and holo- $\Delta 9aa$ bind to the *ureA* and *nikR* promoters at pH 5.8; however, the binding regions are delocalized and hard to define. These experiments at both pH 7.6 and pH 5.8 demonstrate that the N-terminal sequence of HpNikR is required to prevent apoprotein binding to the *ureA* promoter and apo- or holo-protein binding to the *nikR* promoter at pH 7.6, and it also prevents nonspecific binding to both sequences at both pH conditions. In other words, $\Delta 9aa$ does not respond to nickel or pH in the same manner as the full-length protein.

Asp7 and Asp8 Contribution to Specific DNA Binding. Residues 3–11 of HpNikR include two aspartate residues

(at positions 7 and 8) that are likely candidates for pH-responsive components. To test this possibility, both aspartates were simultaneously mutated to alanines, and the DNA-binding activities of the mutant protein were investigated at pH 7.6 and pH 5.8. D7A/D8A HpNikR binds to the *ureA* and *nikR* promoter sequences with comparable affinities as $\Delta 9aa$ in EMSAs ($\sim 10^{-8}$ M, Table 1) and with the same type of protection in the footprinting experiments (Figure 5, Table 2).

To further pinpoint the critical residues, single mutants D7A and D8A were constructed. EMSAs indicate that the single mutants exhibited an affinity similar to that of the wild-type proteins on both the *ureA* and the *nikR* promoters, $\sim 10^{-8}$ M and $\sim 10^{-6}$ M, respectively (Table 1). DNase I footprinting assays also revealed comparable DNA-binding properties and localized binding sites at pH 7.6 and 5.8 as observed for wild-type protein (Figure 6 and data not shown, Table 2), although D7A exhibited slightly tighter affinities. The fact that the single mutants D7A and D8A behave like wild-type HpNikR, in contrast with the double mutant, indicate that for nickel-induced binding to the *ureA* promoter at pH 7.6 and specific DNA recognition on both of the sequences studied, the aspartates do not function as a pair and either one of them can contribute to the DNA-binding response of the protein.

Lys6 Modulation of pH-Responsive DNA Binding. In addition to Asp7 and Asp8, the other charged residue in the N-terminal sequence of HpNikR is Lys6. To provide more information about how this region controls the DNA-binding response to changes in pH, Lys 6 was mutated to alanine. EMSAs reveal that the binding affinity of K6A on the *ureA* promoter (Table 1) is similar to that of the wild-type protein ($\sim 10^{-8}$ M). DNase I footprinting results also demonstrate that, like wild-type, only holo-protein binding is observed on the *ureA* sequence at pH 7.6 while both apo- and holo-K6A-HpNikR bind at pH 5.8 and that under both pH conditions the mutant binds to the same site and with the same affinity as wild-type (Figure S5a of Supporting Information and data not shown, Table 2). In contrast, DNA binding by K6A on the *nikR* promoter at pH 7.6 was not observed in EMSAs (Table 1), and no footprint was detected when up to 10 μ M apo- or holo-K6A was incubated with the *nikR* promoter at pH 7.6 or pH 5.8 (Figure S5b, Supporting Information). These results demonstrate that Lys6 is required for the specific interaction between the HpNikR and the *nikR* promoter, particularly at pH 5.8.

DISCUSSION

Most infectious bacteria cannot survive for long in the human stomach because of the gastric acid, but *H. pylori* not only survive but also flourish there (2). The ability of *H. pylori* to sense and adapt to changes in environmental pH is critical for its survival. However, little is known about what happens in response to acidic shock when the cytoplasmic pH of *H. pylori* appears to drop to pH 4.9–5.8 or how HpNikR might contribute in this situation (4, 35). In the present study, the in vitro metal- and DNA-binding properties of HpNikR at acidic pH were examined to determine if this global activator–repressor can directly respond to changes in pH.

A reduction in the pH from 7.6 to 5.8 does not change the secondary or quaternary structures of HpNikR, and the

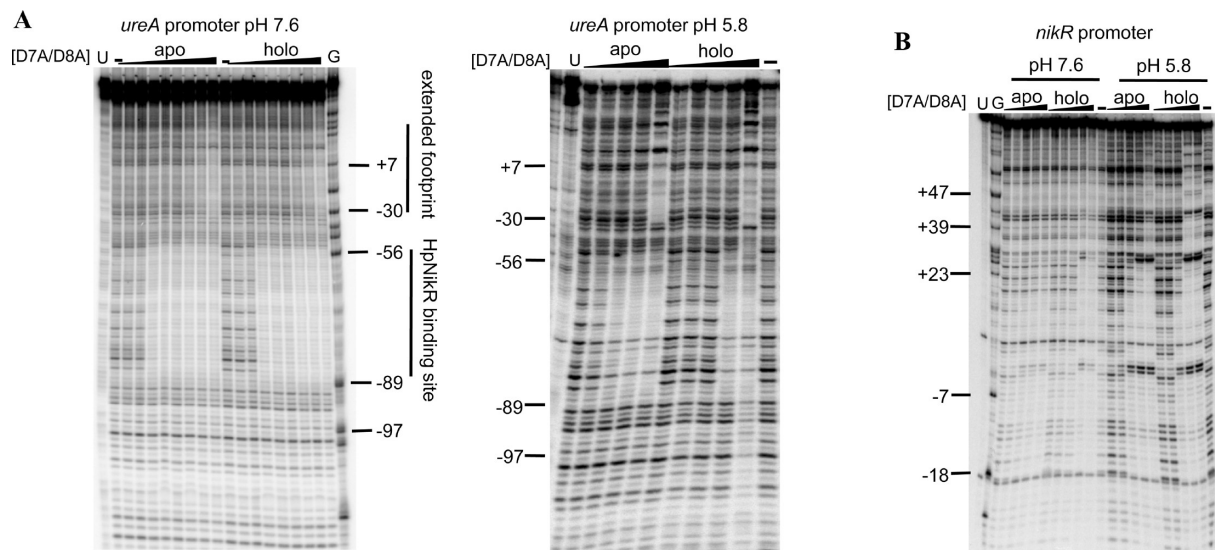


FIGURE 5: D7A/D8A binding to the *ureA* and *nikR* promoters at pH 7.6 and pH 5.8. (A) D7A/D8A binding to the *ureA* promoter at pH 7.6 (left; diluted 1/3 from 10 μ M to 4 nM) and pH 5.8 (right; diluted 1/3 from 1 μ M to 12 nM). (B) D7AD8A (diluted 1/3 from 1 μ M to 12 nM) binding to the *nikR* promoter at pH 7.6 and pH 5.8. Apo- or holo-protein was incubated with the DNA for 30 min prior to the addition of DNase I and analysis on an 8% denaturing polyacrylamide gel. G indicates a Maxam–Gilbert G reaction, and the numbers of the bases are with respect to the transcription start site. U indicates the uncut DNA.

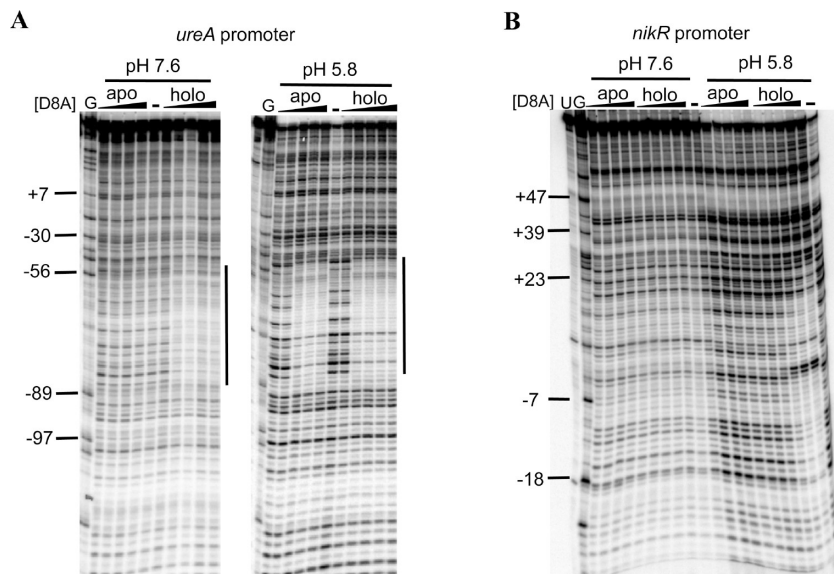


FIGURE 6: D8A binding to the *ureA* and *nikR* promoters at pH 7.6 and pH 5.8. (A) D8A binding to the *ureA* promoter at pH 7.6 (left) and pH 5.8 (right). (B) D8A binding to the *nikR* promoter at pH 7.6 (left) and pH 5.8 (right). Apo- or holo-protein (diluted 1/3 from 1 μ M to 12 nM) was incubated with the DNA for 30 min prior to the addition of DNase I and analysis on an 8% denaturing polyacrylamide gel. G indicates a Maxam–Gilbert G reaction, and the numbers of the bases are with respect to the transcription start site. U indicates the uncut DNA.

electronic absorption spectra suggest that the nickel coordination sphere is not dramatically affected. The nickel-binding affinity of HpNikR is weaker at pH 5.8, but it is still strong enough to induce binding of HpNikR to the *nikR* promoter in a nonlimiting manner. There is some debate about how tightly nickel binds to HpNikR because different methods produce different numbers for the K_D (26, 37). EGTA competition assays monitored by electronic absorption spectroscopy were used to calculate a $K_D \sim 3$ pM for the four nickel ions binding to the HpNikR tetramer at pH 7.6 (26), whereas ITC data were best fit to a two-step nickel-binding process with a $K_D \sim 8$ nM for binding of the first two nickel ions to the tetramer and a $K_D \sim 40$ nM for the last two at pH 7.5 (37). However, regardless of the exact affinity of HpNikR for nickel, it is clear that the affinities of

the nickel sites that stimulate DNA binding are tighter than those of the protein–DNA complexes at either pH. The addition of a large excess of nickel did not affect the apparent DNA affinities in comparison with just stoichiometric amounts of nickel (this study and refs 25, 26, and 38), indicating that quantitative metal binding is achieved at the concentrations of protein that bind DNA. If this were not the case, a tighter apparent DNA binding would be observed in the presence of excess nickel. Several recent studies that monitored HpNikR–DNA binding in the presence of stoichiometric and excess nickel by using EMSA, footprinting assay, and/or ITC are also consistent with the above conclusion (25, 26, 38).

It is known that bacteria can accommodate changes in both external and internal pH by adjusting the transcription of

many different genes such as those involved in the stress response (47). One possible mechanism of this adaptation is through the activity of transcription factors that are directly influenced by pH. For example, the activity of the *E. coli* LexA repressor, which controls multiple genes in the SOS response, is modulated by changes to internal pH in vivo (48). Biochemical experiments revealed that the affinity of LexA for a specific DNA recognition sequence decreases at an acidic pH, but nonspecific DNA binding increases (46, 49), possibly because of changes in the tertiary and quaternary structures of the protein (46). In vitro experiments with the λ cI repressor also demonstrated that lowering the pH had distinct effects on specific binding to several operator sites as well as on nonspecific binding (45, 50), and the results suggested that certain ionizable groups are responsible for distinguishing between DNA sequences but that indirect effects of DNA sequence also contribute to the formation of the protein–DNA complex.

Similarly, changing the pH influences the DNA-binding properties of HpNikR in a manner dependent on the sequence of the DNA target. The binding of HpNikR to the *ureA* promoter is *either* nickel-dependent *or* pH-dependent, and apo- and holo-HpNikR bind to the *ureA* promoter at pH 5.8 with a similar affinity and at the same location as holo-HpNikR at pH 7.6. DNA binding by the apo-form of a metalloregulator that typically exerts its effect through a holo-protein–DNA complex is unusual, but it has also been observed for members of the MerR family of transcription factors (51, 52). In this example, apoprotein binding increases the repression of the already suboptimal promoters, and transcription is activated upon interaction with the metal coregulator that causes a change in the protein–DNA architecture. In the case of HpNikR, whether the combination of reduced pH and nickel binding have a different effect on transcription than the individual signals or whether they represent two separate means to control the activity of HpNikR on the *ureA* promoter is not yet clear. It is possible that nickel and protons each influence binding by HpNikR to the *ureA* DNA sequence through charge redistribution on the protein. This type of model has been suggested for MetJ (53), a RHH protein that responds to the positively charged ligand *s*-adenosylmethionine in the absence of a dramatic protein conformational change (53).

In contrast to the *ureA* sequence, HpNikR binding to the *nikR* sequence is *both* nickel-responsive *and* pH-dependent. In this study, a clear DNase I footprint was only detected on the *nikR* promoter with holo-protein at pH 5.8 but not at pH 7.6, although the recognition sequence is similar to that observed in another study with HpNikR at pH 7.8 (28). The HpNikR protein used in this latter study was left with three extra N-terminal amino acids (GlySerHis) following the removal of an affinity His-tag (28), and it is possible that modification of the N-terminus affects the DNA-binding properties, as observed in this and other studies (25).

One explanation for the formation of the apo-HpNikR–*ureA* and holo-HpNikR–*nikR* complexes upon lowering the pH is a general proton-linked increase in the electrostatic interactions between the protein and the highly charged DNA. However, the observations that pH modulates the DNA complexes on the two promoters in a different manner, that defined binding sites were observed in the DNase I experiments, and that this interaction could not be disrupted with

an excess of nonspecific DNA, indicate that HpNikR binds to the *ureA* and *nikR* promoters at pH 5.8 through specific contacts. In support of this hypothesis, the K6A mutation affects binding to the *nikR* promoter but does not dramatically influence complex formation with the *ureA* sequence, suggesting that there is specific electrostatic interaction between Lys6 and a feature present only in the *nikR* promoter sequence.

It has been proposed that HpNikR acts as a master regulator of acid adaptation by directly mediating acid-induced transcription of *ureA* and possibly other genes that are acid-regulated in *H. pylori* (17, 18, 23, 54, 55). However, the two-component system ArsRS (Hp0165–Hp0166) directly controls acid-induced transcription from the *ureA* promoter in a mechanism that is independent of HpNikR (56). Nevertheless, the ArsR experiments were performed with *H. pylori* cells exposed to pH 5 in the absence of urea, which are conditions that have a small effect on the cytoplasmic pH (4, 35). The DNase I footprinting results shown here likely represent an emergent response of *H. pylori* to extreme acid shock, which would cause a decrease in the cytoplasmic pH (4, 35).

In vivo data suggest that expression of the *nikR* gene increases upon exposure of *H. pylori* to pH 5 without nickel added to the media (17), but it is unclear what factors up-regulate *nikR* expression under those conditions. The DNase I footprinting results described in this report demonstrate that the *nikR* transcription start site is occupied by Ni(II)-HpNikR at pH 5.8, suggesting that HpNikR could repress its own gene expression under acidic shock conditions in the presence of sufficient nickel. Given the nickel affinity of HpNikR ($\sim 10^{-9}$ M) and the relatively weaker binding of Ni(II)-HpNikR to the *nikR* promoter at pH 5.8 ($\sim 10^{-7}$ M), HpNikR autoregulation may place an upper limit on the amount of this protein inside the cell and balance the nickel distribution between several proteins. For example, the down-regulation of HpNikR would limit the level of this potential nickel chelator and allow more nickel to be redirected to apo-urease under acidic conditions when urease activity is required for survival. It may also serve as an indirect method to modulate nickel influx, since Ni(II)-HpNikR represses the expression of the nickel uptake transporter NixA (19, 20).

HpNikR has a very similar structure to the *E. coli* homologue (EcNikR) (16, 32), and the RHH DNA-binding domains from the crystal structures superimpose very well (root mean square deviation, 1.01 Å). However, although the *nikR* promoter in *H. pylori* contains an inverted repeat similar to the EcNikR recognition sequence (33, 41), HpNikR does not bind to the corresponding site (Figure 3D). It was feasible that this difference arises from the extra N-terminal nine amino acids of HpNikR which are not found in EcNikR, especially given that in other members of the RHH family there is an extended region preceding the N-terminal ribbon of the DNA-binding motif which influences DNA binding (57–60). However, removal of this sequence from HpNikR did not result in a shift of the DNA-binding site, suggesting that this is not the critical difference between the two NikR homologues in terms of DNA recognition sequences.

On the other hand, removal of the N-terminal extra nine amino acids of HpNikR does affect the specific DNA-binding response to nickel and pH. Previous work demonstrated that this sequence prevents binding to nonspecific DNA se-

quences in EMSAs (25). Furthermore, Asp7 and Asp8 together are responsible for the specific cation requirement for binding to the *nixA* promoter (25), and it was proposed that the adjacent Asp residues coordinate Mg^{2+} to prevent repulsive electrostatic interactions between the negatively charged Asp residues and the phosphodiester DNA backbone. In the experiments reported here, Asp7 and Asp8 are also observed to prevent apoprotein from binding to the *ureA* promoter at pH 7.6 and nonspecific DNA interactions on the *nikR* promoter at pH 7.6 and both promoters at pH 5.8; however, in this case the two aspartates are redundant, and only one is necessary. These results support the model in which the N-terminal sequences of NikR homologues tune the regulatory capabilities of the proteins by modulating the DNA-binding activities to various sequences and also suggest that they are important for nickel-activated DNA binding to certain sites.

These in vitro results support an intracellular response of *H. pylori* to an extremely acidic environment and provide clues about how HpNikR regulates different operators in response to acid shock. The distinctive pH-responsive DNA binding of HpNikR to the *ureA* and *nikR* promoters also reflects the discriminative strategy of HpNikR-controlled gene regulation. This strategy was recently highlighted by a comparison of many of the promoters regulated by HpNikR (39), which revealed that they can be clearly divided into two separate groups based on the strength of the interaction with HpNikR. Global response regulators often differentially control the expression of genes in response to changes in environmental conditions in order to fine-tune multiple events (61). For example, the DNA binding of another *H. pylori* global regulator, Fur, is either enhanced or diminished in the presence of iron, depending on the promoter, such that iron results in both activation and repression of genes (62). It was suggested that this ability of Fur contributes to the autoregulation of its own gene by an antirepression mechanism that ensures expression of Fur above a minimal threshold (63). Another global response regulator, phosphorylated CtrA from *Caulobacter crescentus*, binds to two promoters with affinities that differ by 10- to 20-fold, which in part results in the temporal control of expression of these genes (64). Future work will determine how HpNikR responds in vivo to external conditions and how they modulate the binding of HpNikR with other promoters to expand our understanding of HpNikR as a global activator–repressor.

ACKNOWLEDGMENT

We thank Harini Kaluarachchi for doing metal analysis. We thank Sheila Wang for critical reading of the manuscript and all members of the Zamble laboratory for helpful discussion.

SUPPORTING INFORMATION AVAILABLE

Site-directed mutagenesis primers, difference electronic absorption spectra, nickel titration of mutants, DNase I footprinting assay titrated with herring sperm DNA, DNase I footprinting assay of K6A with the *ureA* and *nikR* promoters at pH 5.8, and mobility shift assay of $\Delta 9aa$ with the *ureA* and *nikR* promoters. This material is available free of charge via the Internet at <http://pubs.acs.org>.

REFERENCES

- Williamson, J. S. (2001) *Helicobacter pylori*: current chemotherapy and new targets for drug design. *Curr. Pharm. Des.* 7, 355–392.
- Sachs, G., Weeks, D. L., Melchers, K., and Scott, D. R. (2003) The gastric biology of *Helicobacter pylori*. *Annu. Rev. Physiol.* 65, 349–369.
- Stingl, K., Altendorf, K., and Bakker, E. P. (2002) Acid survival of *Helicobacter pylori*: how does urease activity trigger cytoplasmic pH homeostasis? *Trends Microbiol.* 10, 70–74.
- Stingl, K., Uhlemann, E.-M., Schmid, R., Altendorf, K., and Bakker, E. P. (2002) Energetics of *Helicobacter pylori* and its implications for the mechanism of urease-dependent acid tolerance at pH 1. *J. Bacteriol.* 184, 3053–3060.
- Pflock, M., Kennard, S., Finsterer, N., and Beier, D. (2006) Acid-responsive gene regulation in the human pathogen *Helicobacter pylori*. *J. Biotechnol.* 126, 52–60.
- Mobley, H. L. T. (2001) In *Urease, in Helicobacter pylori: Physiology and genetics* (Mobley, H. L. T., Mendz, G. L., and Hazell, S. L., Eds.), pp 179–191, ASM Press, Washington D.C.
- Mulrooney, S. B., and Hausinger, R. P. (2003) Nickel uptake and utilization by microorganisms. *FEMS Microbiol. Rev.* 27, 239–261.
- Olson, J. W., and Maier, R. J. (2002) Molecular hydrogen as an energy source for *Helicobacter pylori*. *Science* 298, 1788–1790.
- Park, K. R., Giard, J.-C., Eom, J. H., Bearson, S., and Foster, J. W. (1999) Cyclic AMP receptor protein and TyrR are required for acid pH and anaerobic induction of *hyaB* and *aniC* in *Salmonella typhimurium*. *J. Bacteriol.* 181, 689–694.
- Vignais, P. M., and Billoud, B. (2007) Occurrence, classification, and biological function of hydrogenases: an overview. *Chem. Rev.* 107, 4206–4272.
- Dosanjh, N. S., and Michel, S. L. J. (2006) Microbial nickel metalloregulation: NikRs for nickel ions. *Curr. Opin. Chem. Biol.* 10, 1–8.
- Maier, R. J., Benoit, S., and Seshadri, S. (2007) Nickel-binding and accessory proteins facilitating Ni-enzyme maturation in *Helicobacter pylori*. *BioMetals* 20, 655–664.
- Belzer, C., Stoof, J., and van Vliet, A. H. (2007) Metal-responsive gene regulation and metal transport in *Helicobacter* species. *BioMetals* 20, 417–429.
- van Vliet, A. H., Poppelaars, S. W., Davies, B. J., Stoof, J., Bereswill, S., Kist, M., Penn, C. W., Kuipers, E. J., and Kusters, J. G. (2002) NikR mediates nickel-responsive transcriptional induction of urease expression in *Helicobacter pylori*. *Infect. Immun.* 70, 2846–2852.
- Contreras, M., Thiberge, J.-M., Mandrand-Berthelot, M.-A., and Labigne, A. (2003) Characterization of the roles of NikR, a nickel-responsive pleiotropic autoregulator of *Helicobacter pylori*. *Mol. Microbiol.* 49, 947–963.
- Schreiter, E. R., and Drennan, C. L. (2007) Ribbon-helix-helix transcription factors: variations on a theme. *Nat. Rev. Microbiol.* 5, 710–720.
- van Vliet, A. H., Kuipers, E. J., Stoof, J., Poppelaars, S. W., and Kusters, J. G. (2004) Acid-responsive gene induction of ammonia-producing enzymes in *Helicobacter pylori* is mediated via a metal-responsive repressor cascade. *Infect. Immun.* 72, 766–773.
- Bury-Moné, S., Thiberge, J.-M., Contreras, M., Maitournam, A., Labigne, A., and De Reuse, H. (2004) Responsiveness to acidity via metal ion regulators mediates virulence in the gastric pathogen *Helicobacter pylori*. *Mol. Microbiol.* 53, 623–638.
- Ernst, F. D., Kuipers, E. J., Heijens, A., Sarwari, R., Stoof, J., Penn, C. W., Kusters, J. G., and van Vliet, A. H. (2005) The nickel-responsive regulator NikR controls activation and repression of gene transcription in *Helicobacter pylori*. *Infect. Immun.* 73, 7252–7258.
- Wolfram, L., Haas, E., and Bauerfeind, P. (2006) Nickel represses the synthesis of the nickel peptidase NixA of *Helicobacter pylori*. *J. Bacteriol.* 188, 1245–1250.
- Ernst, F. D., Stoof, J., Horrevorts, W. M., Kuipers, E. J., Kusters, J. G., and van Vliet, A. H. (2006) NikR mediates nickel-responsive transcriptional repression of the *Helicobacter pylori* outer membrane proteins FecA3 (HP1400) and FrpB4 (HP1512). *Infect. Immun.* 74, 6821–6828.
- Davis, G. S., Flannery, E. L., and Mobley, H. L. T. (2006) *Helicobacter pylori* HP1512 is a nickel-responsive NikR-regulated outer membrane protein. *Infect. Immun.* 74, 6811–6820.

23. van Vliet, A. H., Ernst, F. D., and Kusters, J. G. (2004) NikR-mediated regulation of *Helicobacter pylori* acid adaptation. *Trends Microbiol.* 12, 489–494.
24. Scarlato, V., Delany, I., Spohn, G., and Beier, D. (2001) Regulation of transcription in *Helicobacter pylori*: simple systems or complex circuits? *Int. J. Med. Microbiol.* 291, 107–117.
25. Benanti, E. L., and Chivers, P. T. (2007) The N-terminal arm of the *Helicobacter pylori* Ni²⁺-dependent transcription factor NikR is required for specific DNA binding. *J. Biol. Chem.* 282, 20365–20375.
26. Abraham, L. O., Li, Y., and Zamble, D. B. (2006) The metal- and DNA-binding activities of *Helicobacter pylori* NikR. *J. Inorg. Biochem.* 100, 1005–1014.
27. Atanassova, A., Lam, R., and Zamble, D. B. (2004) A high-performance liquid chromatography method for determining transition metal content in proteins. *Anal. Biochem.* 335, 103–111.
28. Delany, I., Ieva, R., Soragni, A., Hilleringmann, M., Rappuoli, R., and Scarlato, V. (2005) In vitro analysis of protein-operator interactions of the NikR and fur metal-responsive regulators of coregulated genes in *Helicobacter pylori*. *J. Bacteriol.* 187, 7703–7715.
29. Fauquant, C., Diederix, R. E. M., Rodrigue, A., Dian, C., Kapp, U., Terradot, L., Mandrand-Berthelot, M. A., and Michaud-Soret, I. (2006) pH dependent Ni(II) binding and aggregation of *Escherichia coli* and *Helicobacter pylori* NikR. *Biochimie* 88, 1693–1705.
30. Bloom, S. L., and Zamble, D. B. (2004) Metal-selective DNA-binding response of *Escherichia coli* NikR. *Biochemistry* 43, 10029–10038.
31. Chivers, P. T., and Sauer, R. T. (2002) NikR repressor: high-affinity nickel binding to the C-terminal domain regulates binding to operator DNA. *Chem. Biol.* 9, 1141–1148.
32. Dian, C., Schauer, K., Kapp, U., McSweeney, S. M., Labigne, A., and Terradot, L. (2006) Structural basis of the nickel response in *Helicobacter pylori*: crystal structures of HpNikR in Apo and nickel-bound states. *J. Mol. Biol.* 361, 715–730.
33. Schreiter, E. R., Wang, S. C., Zamble, D. B., and Drennan, C. L. (2006) NikR-operator complex structure and the mechanism of repressor activation by metal ions. *Proc. Natl. Acad. Sci. U.S.A.* 103, 13676–13681.
34. Sambrook, J., and Russell, D. W. (2001) *Molecular cloning: A laboratory manual*, Cold Spring Harbor Laboratory Press, New York.
35. Stingl, K., Uhlemann, E.-M., Deckers-Hebestreit, G., Schmid, R., Bakker, E. P., and Altendorf, K. (2001) Prolonged survival and cytoplasmic pH homeostasis of *Helicobacter pylori* at pH 1. *Infect. Immun.* 69, 1178–1181.
36. Dosanjh, N. S., Hammerbacher, N. A., and Michel, S. L. (2007) Characterization of the *Helicobacter pylori* NikR-P(ureA) DNA interaction: metal ion requirements and sequence specificity. *Biochemistry* 46, 2520–2529.
37. Zambelli, B., Bellucci, M., Danielli, A., Scarlato, V., and Ciurli, S. (2007) The Ni²⁺ binding properties of *Helicobacter pylori* NikR. *Chem. Commun. (Cambridge, U.K.)* 3649–3651.
38. Zambelli, B., Danielli, A., Romagnoli, S., Neyroz, P., Ciurli, S., and Scarlato, V. (2008) High-affinity Ni²⁺ binding selectively promotes binding of *Helicobacter pylori* NikR to its target urease promoter. *J. Mol. Biol.* 383, 1129–1143.
39. Dosanjh, N. S., West, A. L., and Michel, S. L. (2009) *Helicobacter pylori* NikR's Interaction with DNA: A Two-Tiered Mode of Recognition. *Biochemistry* 48, 527–536.
40. Schreiter, E. R., Sintchak, M. D., Guo, Y., Chivers, P. T., Sauer, R. T., and Drennan, C. L. (2003) Crystal structure of the nickel-responsive transcription factor NikR. *Nat. Struct. Biol.* 10, 794–799.
41. Chivers, P. T., and Sauer, R. T. (2000) Regulation of high affinity nickel uptake in bacteria. *J. Biol. Chem.* 275, 19735–19741.
42. Cun, S., Li, H., Ge, R., Lin, M. C., and Sun, H. (2008) A histidine-rich and cysteine-rich metal-binding domain at the C terminus of heat shock protein A from *Helicobacter pylori*: implication for nickel homeostasis and bismuth susceptibility. *J. Biol. Chem.* 283, 15142–15151.
43. Zeng, Y.-B., Zhang, D.-M., Li, H., and Sun, H. (2008) Binding of Ni(2+) to a histidine- and glutamine-rich protein, Hpn-like. *J. Biol. Inorg. Chem.* 13, 1121–1131.
44. Li, L., von Kessler, D., Beachy, P. A., and Matthews, K. S. (1996) pH-dependent enhancement of DNA binding by the ultrathorax homeodomain. *Biochemistry* 35, 9832–9839.
45. Senear, D. F., and Ackers, G. K. (1990) Proton-linked contributions to site-specific interactions of λ cI repressor and O_R. *Biochemistry* 29, 6568–6577.
46. Sousa, F. J., Lima, L. M. T. R., Pacheco, A. B. F., Oliveira, C. L. P., Torriani, I., Almeida, D. F., Foguel, D., Silva, J. L., and Mohana-Borges, R. (2006) Tetramerization of the LexA repressor in solution: implications for gene regulation of the *E. coli* SOS system at acidic pH. *J. Mol. Biol.* 359, 1059–1074.
47. Olson, E. R. (1993) Influence of pH on bacterial gene expression. *Mol. Microbiol.* 8, 5–14.
48. Dri, A.-M., and Moreau, P. L. (1994) Control of the LexA regulon by pH: evidence for a reversible inactivation of the LexA repressor during the growth cycle of *Escherichia coli*. *Mol. Microbiol.* 12, 621–629.
49. Relan, N. K., Jenuwine, E. S., Gumbs, O. H., and Shaner, S. L. (1997) Preferential interactions of the *Escherichia coli* LexA repressor with anions and protons are coupled to binding the *recA* operator. *Biochemistry* 36, 1077–1084.
50. Senear, D. F., and Batey, R. (1991) Comparison of operator-specific and nonspecific DNA binding of the λ cI repressor: [KCl] and pH effects. *Biochemistry* 30, 6677–6688.
51. Brown, N. J., Stoyanov, J. V., Kidd, S. P., and Hobman, J. L. (2003) The MerR family of transcriptional regulators. *FEMS Microbiol. Rev.* 27, 145–163.
52. Outten, F. W., Outten, C. E., and O'Halloran, T. V. (2000) in *Metalloregulatory systems at the interface between bacterial metal homeostasis and resistance*, in *Bacterial Stress Responses* (Storz, G., and Hengge-Aronis, R., Eds.), pp 145–157, ASM Press, Washington D.C.
53. Phillips, K., and Phillips, S. E. (1994) Electrostatic activation of *Escherichia coli* methionine repressor. *Structure* 2, 309–316.
54. Merrell, D. S., Goodrich, M. L., Otto, G., Tompkins, L. S., and Falkow, S. (2003) pH-regulated gene expression of the gastric pathogen *Helicobacter pylori*. *Infect. Immun.* 71, 3529–3539.
55. Scott, D. R., Marcus, E. A., Wen, Y., Oh, J., and Sachs, G. (2007) Gene expression in vivo shows that *Helicobacter pylori* colonizes an acidic niche on the gastric surface. *Proc. Natl. Acad. Sci. U.S.A.* 104, 7235–7240.
56. Pflock, M., Kennard, S., Delany, I., Scarlato, V., and Beier, D. (2005) Acid-induced activation of the urease promoters is mediated directly by the ArsRS two-component system of *Helicobacter pylori*. *Infect. Immun.* 73, 6437–6445.
57. Raumann, B. E., Rould, M. A., Pabo, C. O., and Sauer, R. T. (1994) DNA recognition by β -sheets in the Arc repressor-operator crystal structure. *Nature* 367, 754–757.
58. Somers, W. S., and Phillips, S. E. (1992) Crystal structure of the met repressor-operator complex at 2.8 Å resolution reveals DNA recognition by beta-strands. *Nature* 359, 387–393.
59. Raumann, B. E., Brown, B. M., and Sauer, R. T. (1994) Major groove DNA recognition by β -sheets: the ribbon-helix-helix family of gene regulatory proteins. *Curr. Opin. Struct. Biol.* 4, 36–43.
60. Knight, K. L., and Sauer, R. T. (1989) Identification of functionally important residues in the DNA binding region of the *mnt* repressor. *J. Biol. Chem.* 264, 13706–13710.
61. Foster, P. L. (2007) Stress-induced mutagenesis in bacteria. *Crit. Rev. Biochem. Mol. Biol.* 42, 373–397.
62. Delany, I., Spohn, G., Rappuoli, R., and Scarlato, V. (2001) The Fur repressor controls transcription of iron-activated and -repressed genes in *Helicobacter pylori*. *Mol. Microbiol.* 42, 1297–1309.
63. Delany, I., Spohn, G., Rappuoli, R., and Scarlato, V. (2003) An anti-repression Fur operator upstream of the promoter is required for iron-mediated transcriptional autoregulation in *Helicobacter pylori*. *Mol. Microbiol.* 50, 1329–1338.
64. Reisenauer, A., Quon, K., and Shapiro, L. (1999) The CtrA response regulator mediates temporal control of gene expression during the *Caulobacter* cell cycle. *J. Bacteriol.* 181, 2430–2439.

BI801742R